

Coordination Chemistry of Ir with Chelating Ligands Containing a Xanthine-Derived, Protic N-Heterocyclic Carbene (NHC) Moiety

Matteo Bevilacqua,^[a] Valerio Giuso,^[a] Marzio Rancan,^[b, c] Lidia Armelao,^[a, b, c] Claudia Graiff,^[d] Walter Baratta,^[e] Valerio Di Marco,^[a] and Andrea Biffis*^[a, c]

A series of protic N-heterocyclic carbene ligand precursors based on theophylline or adenine has been prepared, and the reactivity and coordination chemistry of these proligands towards iridium(III) centers has been investigated. Complex formation appears to be highly dependent on the proligand

structure. In one case, a particularly stable complex is formed that enables fully reversible protonation/deprotonation of the coordinated NHC moiety. The acidity constant of the protonated complex was consequently determined.

Introduction

One of the reasons for the ongoing interest for N-Heterocyclic Carbenes (NHCs)^[1] as ligands towards metal complexes is the intriguing possibility that such complexes can spontaneously form *in vivo* under given circumstances and that they can consequently play a role in cell metabolism.^[2] Indeed, proteins (through amino acids such as histidine) and nucleic acids (through nucleobases such as adenine or guanine) contain imidazole or purine heterocycles that can be transformed into NHC complexes by reaction with suitable metal centers. Such

transformations might involve tautomerization of the heterocycle to the generally disfavored carbene form, which becomes stabilized by coordination to the metal center (Scheme 1, reaction a)).^[3] Alternatively, oxidative addition/reductive elimination sequences involving the procarbenic C–H (usually C-2 in imidazoles and C-8 in purines) can be exploited (Scheme 1, reaction b)).^[4] Finally, sigma bond metathesis or concerted metalation deprotonation (CMD) pathways, assisted by free bases or basic ligands at metal and followed by protonation of the resulting anionic NHC^[5] may also take place (Scheme 1, reaction c)); the first step of this last sequence is particularly well established in the context of catalytic reactions leading to the direct arylation of these heterocycles at the procarbenic carbon.^[6] Through these pathways, a peculiar class of NHC ligands bound to metal centers is formed, the so-called “protic” NHCs, in which at least one of the substituents at the wingtip nitrogen atoms of the NHC is a hydrogen.^[7]

Several protic NHC ligands of this kind have already been reported, though mostly starting from simple model heterocycles such as imidazole or benzimidazole rather than from histidine, purines or other suitable N-heterocyclic biocompounds such as those belonging to the xanthine family.^[8]

[a] M. Bevilacqua, V. Giuso, Prof. L. Armelao, Prof. V. Di Marco, Prof. A. Biffis

Dipartimento di Scienze Chimiche
Università di Padova
Via Marzolo 1, 35131 Padova, Italy
E-mail: andrea.biffis@unipd.it
www.organometallics.it

[b] Dr. M. Rancan, Prof. L. Armelao

Institute of Condensed Matter Chemistry and Technologies for Energy (ICMATE)
National Research Council (CNR)
Via Marzolo 1, 35131 Padova, Italy

[c] Dr. M. Rancan, Prof. L. Armelao, Prof. A. Biffis

Consorzio Interuniversitario per le Reattività Chimiche e la Catalisi (CIRCC)
c/o Dipartimento di Scienze Chimiche
Università di Padova
Via Marzolo 1, 35131 Padova, Italy

[d] Prof. C. Graiff

Dipartimento di Scienze Chimiche, della Vita e della Sostenibilità Ambientale
Università di Parma
Parco Area delle Scienze 17/A, 43124 Parma, Italy

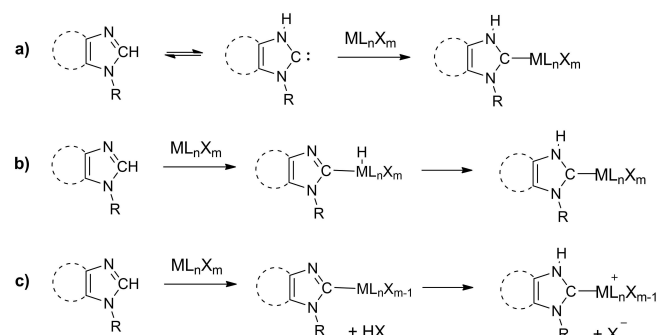
[e] Prof. W. Baratta

Dipartimento di Scienze Agroalimentari, Ambientali e Animali
Università di Udine
Via Cotonificio 108, 33100 Udine, Italy

Supporting information for this article is available on the WWW under <https://doi.org/10.1002/ejic.202200484>

Part of the Institute Feature highlighting the “Interuniversity Consortium in Chemical Reactivity and Catalysis (CIRCC)”.

© 2022 The Authors. European Journal of Inorganic Chemistry published by Wiley-VCH GmbH. This is an open access article under the terms of the Creative Commons Attribution License, which permits use, distribution and reproduction in any medium, provided the original work is properly cited.



Scheme 1. Mechanistic pathways leading to metal complexes with protic NHCs from free heterocyclic precursors.

Furthermore, the peculiar properties of these ligands, i.e. the possibility of being reversibly deprotonated,^[9] their capability to form hydrogen bonds with substrates,^[10] and to act cooperatively with the metal center in stoichiometric and catalytic reactions^[11] have been envisaged but very scarcely exploited up to now. This is at odds with the extensive studies that have been conducted using some N-heterocyclic biocompounds, in particular purines or xanthines such as theophylline, theobromine or caffeine, as N-donor ligands^[12] or as more conventional NHC ligands, produced upon alkylation at both nitrogen atoms in the five membered ring and subsequent deprotonation.^[13]

In this work, we would like to contribute to filling this gap and consequently to investigate on the preparation of potential bi- and tridentate ligands containing protic NHCs deriving from theophylline or adenine and on their coordination chemistry with Cp*Ir(III) centers. The properties of the resulting robust chelate complexes, which derive from the reversible ligand deprotonation, will be quantitatively investigated, as they may potentially lead to a peculiar behavior of these compounds in molecular recognition, sensing, catalysis, and biomedicine.^[14,15]

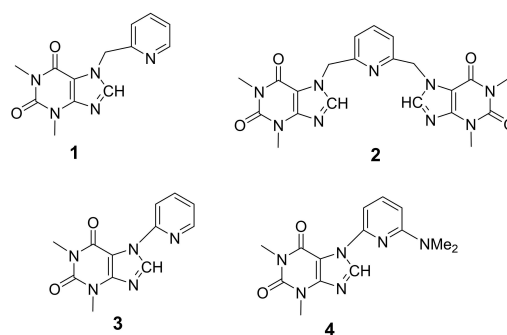
Results and Discussion

We have begun our investigation by synthesizing a small library of precursors of protic NHCs starting from theophylline (Scheme 2). Precursor **1** was previously reported in the literature,^[8k] whereas precursors **2–4** are novel compounds.

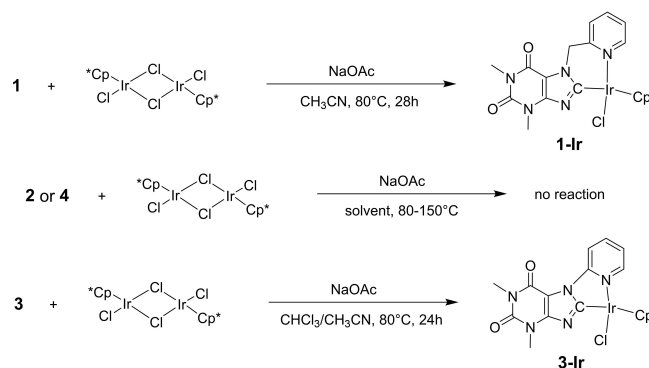
Nucleophilic substitution by theophylline on 2-bromomethyl- or 2,6-bis(bromomethyl)-pyridine yields the literature-known precursor **1** as well as the novel di-NHC precursor **2** (Scheme 3, reactions a and b). Theophylline invariably attacks the electrophilic substrate with the nitrogen atom in position 7 of the heterocycle, which is more nucleophilic and less sterically encumbered (no methyl group in beta position). Similarly,



Andrea Biffis graduated in Chemistry (honors) at the University of Padova (with Prof. Benedetto Corain) and received his PhD in 1998 from the University of Düsseldorf, Germany (with Prof. Günter Wulff). After a postdoctoral stay at the University of Essen, Germany (with Prof. Günter Schmid), he returned to Padova, where he was appointed assistant professor in 2001, associate professor in 2011 and full professor in 2022. Prof. Biffis has at present coauthored more than 110 ISI publications in peer-reviewed international journals and 6 chapters in monographs, with a Hirsch index *h* equal to 36 (source: Scopus). The research interests of Prof. Biffis deal mainly with the development of late transition metal catalysts (metal nanoparticles, metal complexes) for the synthesis of fine chemicals, as well as with the implementation of strategies for catalyst recovery and recycling, employing biphasic systems or soluble crosslinked polymers (microgels) as catalyst support.



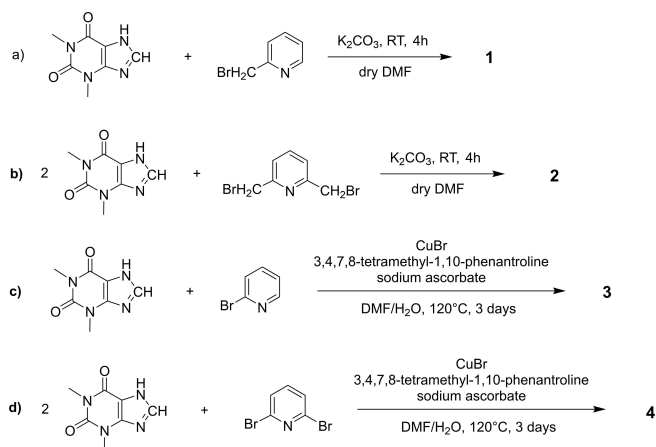
Scheme 2. Theophylline-based proligands employed in this work.



Scheme 3. Preparation of the theophylline-based proligands 1–4.

Ullmann-type coupling of theophylline with 2-bromopyridine yields precursor **3** (Scheme 3 reaction c); despite the mechanistic differences between these two reactions, arylation takes place also in this case at position 7 of the ring, which is again dictated by steric and electronic factors. The analogous reaction with 2,6-dibromopyridine instead does not furnish the corresponding di-NHC precursor. Apparently, reaction of the second C–Br bond with theophylline is disfavored, whereas a competitive reaction with dimethylamine takes place, that is inevitably present in the reaction system due to slight decomposition of DMF solvent under reaction conditions. The reaction consequently yields precursor **4** (Scheme 3, reaction d) that was included in the screening. Other solvents not undergoing decomposition with amine formation, such as N-methylpyrrolidinone, were tested as alternative solvents, but the second C–N coupling reaction did not proceed in these cases. All precursors were purified and characterized spectroscopically and exhibited the expected spectral features (see the Supporting Information for details).

We then turned to the use of these proligands for the preparation of iridium(III) complexes, upon reaction with the conventional precursor $[(\text{IrCp}^*(\mu\text{-Cl})\text{Cl})_2]$. Reaction of this precursor with proligand **1** was already reported by the group of Hahn^[13] and yielded complex **1-Ir** (Scheme 4), in which the xanthine moiety turns into an anionic NHC ligand. We were able to reproduce Hahn's results in this respect, obtaining the expected complex.



Scheme 4. Strategy for the preparation of Ir(III) complexes described in this work.

We then attempted the same reaction with proligands 2–4, with mixed results. Reaction of proligand 2 was severely hampered by its rather poor solubility in all nonaqueous solvents, and despite several attempts with alternative solvents (N,N-dimethylformamide) and higher reaction temperatures (up to 150 °C) the reaction invariably resulted in the recovery of the starting proligand. On the other hand, proligand 3 promptly yielded the corresponding Ir(III) complex 3-Ir in high yield and shorter reaction times compared to proligand 1, whereas proligand 4 turned out to be soluble but completely unreactive and was recovered intact after reaction. We speculate that the presence of the dimethylamino group in 6-position hampers the reactivity of proligand 4 because it inhibits the coordination of the Ir precursor to the pyridine nitrogen through both electronic and steric effects. Remarkably, these reactions do not proceed in the absence of sodium acetate, which points towards a CMD mechanism for complex formation and justifies the fact that no protonation of the anionic NHC ligand to the corresponding protic NHC is observed.

The newly synthesized complex 3-Ir was spectroscopically characterized by multinuclear NMR and exhibited the expected features, such as the disappearance of the signal of the procarbenic hydrogen in position 8 of the xanthine ring and the extensive downfield shift experienced by the signals of the pyridine hydrogens. In the ¹³C spectrum of the complex, C-8, which is coordinated to Ir, is significantly deshielded and resonates at 173.9 ppm, which is a chemical shift fully comparable to that recorded in conventional, neutral NHC ligands derived from N,N'-difunctionalized theophyllinium cations.^[13] This observation lends support to the interpretation of this anionic azolate ligand as a carbene ligand, in which the anionic charge is largely found on the unsubstituted nitrogen atom and on the ligand backbone, rather than on C-8 (see also below).

The complex was recrystallized by diffusion of diethyl ether vapors into a chloroform solution and its crystal structure was determined (Figure 1). Selected bond lengths and angles are

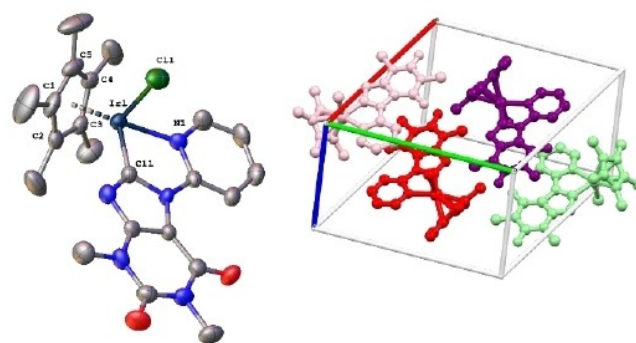
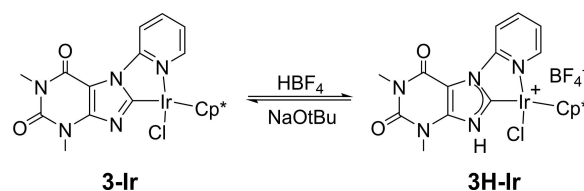


Figure 1. Asymmetric unit and unit cell of compound 3-Ir. Anisotropic displacement ellipsoids for the non-H atoms are displayed at the 50% probability level. Color code: Ir dark blue, Cl green, O red, N light blue, C grey. H-atoms are omitted for clarity. Selected bond distances and angles [Å and deg]: Cp–Ir1 1.821(10), C11–Ir1 1.997(4), Cl1–Ir1 2.3965(12), N1–Ir1 2.083(4), Cl1–Ir1–N1 85.68(10), N1–Ir1–C11 77.32(15), Cl1–Ir1–C11 90.48(12), Cp–Ir1–Cl1 124.28(3), Cp–Ir1–N1 132.63(9), Cp–Ir1–C11 130.51(12).

listed in the figure caption and crystallographic data are shown in Table S1 in the Supporting Information.

Compound 3-Ir crystallizes in the *P*₂/*c* monoclinic space group with four molecules per unit cell (*Z* = 4). The complex displays the typical half-sandwich “three-legged piano-stool” geometry. In this pseudo-octahedral geometry, the metal binds a Cp* ligand (Ir1 to Cp* centroid distance 1.821 Å), a chloride anion (Ir1–Cl1 2.396 Å) and the chelating N–C ligand deriving from 3 (Ir1–C11 1.987 Å and Ir1–N1 2.083 Å). Concerning the anionic NHC moiety, it is interesting to remark that the two C–N distances in the imidazole ring are significantly different: the one with the unsubstituted N being shorter (1.334 vs. 1.388 Å). This observation has been already made in the past in other metal complexes with anionic NHCs of the same kind and found to be dependent on the obviously different character of the two nitrogen atoms, while the metal-bound carbon maintains its carbene character; this is supported by theoretical calculation demonstrating that no excess anionic charge is present on the carbene atom, whereas the charge is rather concentrated on the unsubstituted nitrogen.^[5]

Both NMR characterization and structural analysis confirm that the xanthine-derived ligand in complex 3-Ir is formally an LX type ligand and exhibits a free nitrogen with basic character that is not protonated during the synthesis, as expected in view to the basic conditions employed. We then verified the possibility to protonate this nitrogen generating the corresponding protic NHC ligand (Scheme 5). Treatment of a chloro-



Scheme 5. Reversible protonation of complex 3-Ir.

form solution of complex **3-Ir** with an ethereal HBF_4 solution causes the immediate precipitation of a solid that turned out to be the protonated complex **3H-Ir**.

The NMR spectroscopic features of the complex change significantly upon protonation. First of all, the signal of the imidazolic N–H is recorded as a broad singlet at 11.60 ppm. The signals of the pyridine hydrogen become significantly deshielded upon protonation, whereas the signals of the Cp^* ring are largely unaffected. The signal of C-8 in the ^{13}C NMR spectrum also remains largely unaffected by protonation and resonates at 174.7 ppm compared to 173.9 ppm in the unprotonated complex **3-Ir**. Again, this supports the interpretation of the theophylline moiety acting through C-8 as a carbene ligand in both cases.

The crystal structure of **3H-Ir** was also determined (Figure 2). In the crystal structure of compound **3H-Ir** two cationic complexes, two BF_4^- anions and solvent molecules are present. The two metal complexes are crystallographically independent but very similar. The metal atom is tetrahedrally coordinated considering the centroid of the Cp^* ring, the chloride, the carbene atom of the theophylline and the nitrogen atom of the pyridine moiety. The compound is chiral but, in the crystals, both enantiomers are present, being *P*-1 a centrosymmetric space group. The theophylline and the pyridine systems are almost coplanar, the dihedral angle is 11.16° and 10.93° in the two cations. The protonation on the imidazole unit allows hydrogen bonds with the chlorine atom between the two cationic molecules (the distances $\text{N}\cdots\text{Cl}$ are 3.150 and 3.157 Å and the $\text{N}-\text{H}\cdots\text{Cl}$ angles are 144.86° and 145.60°); moreover, a $\pi\cdots\pi$ stacking interaction can be observed between the ligands with a distance from centroid to centroid of the imidazole rings of 3.546 Å, leading to the formation of dimers.

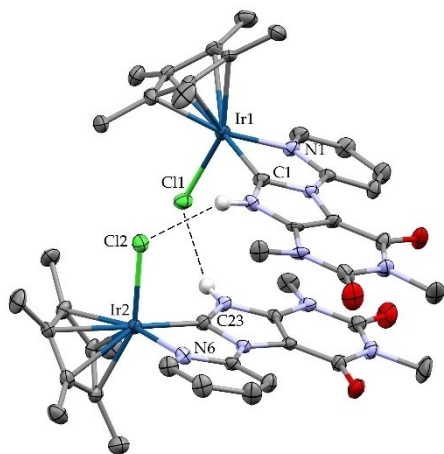


Figure 2. Molecular structure of the two cationic complexes in **3H-Ir**, evidencing the formation of dimers. Ellipsoids are depicted at their 30% probability level. Anions and hydrogen atoms are omitted for clarity excepting the hydrogen atom on the imidazole moieties. Selected bond distances and angles [Å and deg]: Cp–Ir1 1.838(10), C1–Ir1 1.998(16), Cl1–Ir1 2.424(4), Ir1–N1 2.110(13), C23–Ir2 1.847(11), C23–Ir2 1.987(15), Cl2–Ir2 2.427(4), Ir2–N6 2.116(13); C1–Ir1–N1 $75.6(5)$, C1–Ir1–Cp $131.3(6)$, N1–Ir1–Cp $131.0(6)$, C1–Ir1–Cl1 $94.3(5)$, N1–Ir1–Cl1 $87.9(4)$, Cp–Ir1–Cl1 $121.9(5)$, C23–Ir2–N6 $76.2(6)$, C23–Ir2–Cp $130.8(6)$, N6–Ir2–Cp $129.9(6)$, C23–Ir2–Cl2 $94.6(5)$, N6–Ir2–Cl2 $88.3(4)$, Cp–Ir2–Cl2 $122.6(5)$.

Concerning the NHC moiety, the differences with the deprotonated complex **3-Ir** are significant. The two N–C bond distances in the imidazole ring are now as expected much more similar (1.357 and 1.369 Å for the alkylated and protonated nitrogen, respectively) and the NCN bond angle also reduces from 110.94° to 105.45° .

We have verified that protonation of **3-Ir** was reversible. Indeed, treatment of **3H-Ir** with one equivalent of $t\text{BuONa}$ restored complex **3-Ir**. Once we proved the stability of both complexes **3-Ir** and **3H-Ir**, as well as the reversibility of the protonation process, we were ready to study the protonation in more quantitative terms, with the aim to extract information such as the acidity constant of complex **3H-Ir**. In order to determine this parameter, we chose the approach of performing a spectroscopic titration of **3-Ir** with controlled additions of HBF_4 . Initially, we wanted to perform the spectroscopic titration in water-rich acetonitrile–water mixture, in order to determine the acidity constant of the complex more directly and precisely. However, we had to realize that upon addition of excess water the UV-Vis spectrum of **3-Ir** changed significantly, even without acid addition, and was not further modified by subsequent additions of acid. We attribute this behavior to the dissociation of the chlorido ligand, which is favored by a water-rich environment, with formation of a monocationic Ir complex completing its coordination sphere with a molecule or water or acetonitrile. This complex, being already monocationic, is not easily protonated by the acid, since it would become dicationic. On the basis of the above, we decided to perform the spectroscopic titration in pure acetonitrile. The experimental setup was to start with a solution of complex **3-Ir** in acetonitrile and then to add well defined portions of an HBF_4 solution in acetonitrile, recording the UV-Vis spectrum of the solution after each addition and accounting also for the resulting dilution. The sequence of the obtained UV-Vis spectra is reported in Figure 3. It can be appreciated that there is a smooth transition

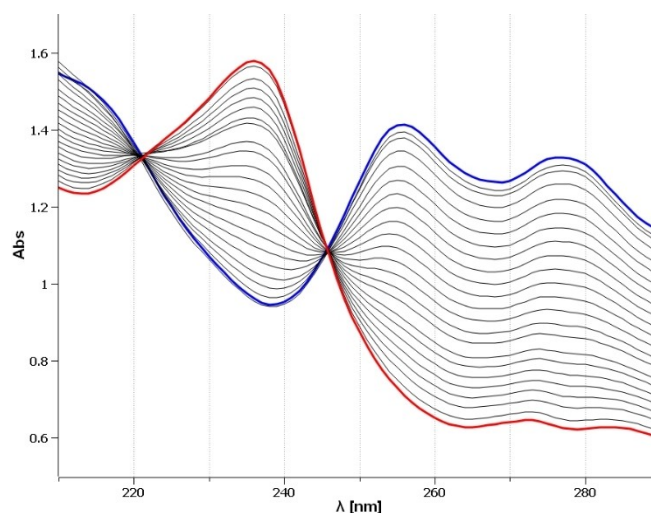


Figure 3. UV-Vis titration of complex **3-Ir** with $\text{HBF}_4\cdot\text{Et}_2\text{O}$. (0.0425 eq. H^+ per addition): blue spectrum before acid addition, red spectrum after addition of 0.93 eq. H^+).

from the UV-Vis spectrum of complex **3-Ir** (blue spectrum in Figure 3) to the spectrum of complex **3H-Ir** (red spectrum). Furthermore, the two isobestic points suggest indeed the presence of an equilibrium between the two species.

These data were fitted through a proper model (see the Supporting Information for details) which allowed to determine the acidity constant for complex **3H-Ir** ($pK_a = 7.6 \pm 0.2$), as well as its actual purity (which resulted to be slightly less than 100%, i.e. $93.6 \pm 0.4\%$) and the molar absorptivities of the two complexes at different wavelengths (which are reported in Table 1).

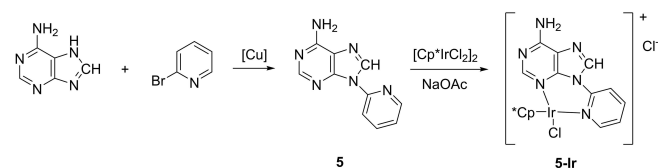
The possibility to perform reversible protonation/deprotonation reactions was evaluated also with complex **1-Ir**. Treatment of a chloroform solution of this complex with a HBF_4 solution did not actually produce the formation of a precipitate. Solvent evaporation resulted in the formation of an oil that indeed exhibited spectroscopic features compatible with a complete protonation of the free nitrogen, hence with formation of a **1H-Ir** complex. However, when this oil was treated with diethyl ether to remove residual acid and promote its solidification, the solid that was generated exhibited a different NMR spectrum, in which all complex signals were split in two, pointing to the formation of dimers. Unfortunately, we have been up to now unable to grow crystals of this compound, hence we do not know the exact structure of these dimers. Without this information, it is also not possible for the moment to conduct spectroscopic titrations with this compound.

Given the successful synthesis of complexes **3-Ir/3H-Ir** and their recorded stability, we considered to investigate the coordination chemistry of other ligand precursors with similar structure but derived from simple xanthine or adenine as the protic NHC precursors. Reaction of xanthine with 2-bromopyridine was however prevented by the very low solubility of this heterocycle in all the considered reaction solvents. Reaction of adenine with 2-bromopyridine using reaction conditions similar to those employed for the preparation of **3** yielded instead the arylation product **5** in good yields (Scheme 6), in which stereo-electronic factors favored arylation at position 9 of the ring.

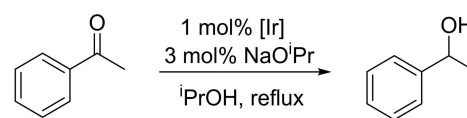
Reaction of **5** with Ir provided a product in good yields, which was however not the expected one. Indeed, the proli-

Table 1. Estimated molar absorptivities of complexes **3-Ir** and **3H-Ir** at various wavelengths in acetonitrile.

λ [nm]	ϵ 3-Ir	ϵ 3H-Ir
236	12170 ± 50	27990 ± 80
256	21170 ± 90	12260 ± 80
277	19960 ± 90	10780 ± 70



Scheme 6. Synthesis of proligand **5** and complex **5-Ir**.



Scheme 7. Transfer hydrogenation of acetophenone catalyzed by complexes **1-Ir** and **5-Ir**.

gand was not deprotonated at C-8 and acted instead apparently as an L_2 -type ligand with two nitrogen atoms towards the Ir center, presumably forming complex **5-Ir** (Scheme 6). Such a behavior was already observed with similar proligands by the group of Hahn.^[8n] They were however able to switch the coordination mode of the proligand by heating up the reaction mixture. This procedure unfortunately was not successful in our case.

Finally, the catalytic performance of complexes **1-Ir** and **3-Ir** was preliminarily evaluated. A standard test reaction, such as the transfer hydrogenation of acetophenone (Scheme 7) was selected. Only the unprotonated complexes **1-Ir** and **3-Ir** were considered, given the employed strongly basic reaction conditions. Complex **3-Ir** was able to reach 62% yield in 1-phenylethanol after 30 hours reaction time and 99% yield after 95 hours ($\text{TOF } 2 \text{ h}^{-1}$ at 50% conversion). On the other hand, complex **1-Ir** was less efficient and was able to convert acetophenone only partially (40% reaction yield after 90 hours). Thus, complex **3-Ir** appears markedly superior as catalyst, though its performance is currently far below that of the best iridium based catalysts for this reaction.^[16]

Conclusion

We have successfully prepared complexes of iridium(III) with chelating ligands bearing a protic NHC moiety derived from theophylline and a pyridyl group as side arm. Ligands with a direct bond between the xanthine moiety and the pyridine group appear to afford more stable complexes that can reversibly undergo protonation at N9. Work is now in progress to expand this synthetic strategy and especially to further evaluate the properties of the resulting Ir complexes in catalysis and medicine field.

Experimental Section

Synthesis of ligand 3. A 10 ml pressure tube was filled with theophylline (913.8 mg, 5.07 mmol), CuBr (39.4 mg, 0.27 mmol), sodium ascorbate (109.0 mg, 0.55 mmol), KOH (501.4 mg, 8.93 mmol), 3,4,7,8-tetramethyl-1,10 phenanthroline (117.5 mg, 0.49 mmol). Three argon-vacuum cycles were carried out with the aid of a silicone septum before, finally, a solution of 2-bromopyridine (750 μL , 7.55 mmol), in 10 mL di DMF/ H_2O 4:1 was injected and the sealed tube was left under stirring at 120°C for 3 days. The resulting brown solid was taken up in a little chloroform and filtered on a glass frit. The brown solution is evaporated under reduced pressure to a brown oil which can be purified by extraction using ethyl acetate/hexane (2/1). The ligand can also be purified by

column chromatography on silica using ethyl acetate/hexane (2/1) as eluent. The product, which appears as a white solid, was used without further purification. Yield 849 mg (77%). Yield 134 mg (51%). $^1\text{H NMR}$ (CDCl_3): δ 3.47 (s, 3H, CH_3), 3.69 (s, 3H, CH_3), 7.41 (m, 1H, *m*-CH pyr), 7.92 (td, 1H, *p*-CH pyr), 8.07 (d, 1H, *m*-CH pyr), 8.48 (s, 1H, theophylline), 8.53 (d, 1H, *o*-CH pyr). $^{13}\text{C NMR}$ (CDCl_3): δ 29.5 (CH_3), 31.0 (CH_3), 106.8 (NC(CO)) 119.5 (pyr), 124.5 (pyr), 139.7 (pyr), 142.9 (NCHN), 148.5 (pyr), 149.5 (pyr), 151.7 (CO), 152.3 (NCN), 155.5 (CO). Elemental analysis (%) calc for $\text{C}_{12}\text{H}_{11}\text{N}_5\text{O}_2$: C 56.03; H 4.31; N 27.22. Found: C 55.93; H 4.25; N 26.47.

Synthesis of complex **3-Ir**. [$\text{IrCp}^*(\mu\text{-Cl})\text{Cl}$] $_2$ (105.8 mg, 0.1328 mmol), proligand **3** (66.9 mg, 0.260 mmol) and sodium acetate trihydrate (133.3 mg, 0.979 mmol) were placed in a Schlenk tube. The tube was disereated with three argon-vacuum cycles, and then 4 ml $\text{CHCl}_3\text{:CH}_3\text{CN}$ 1:1 were added. The resulting orange solution was then heated under stirring at 80 °C for 16 hours. The resulting red solution is filtered on Celite, and the solid residue is washed with 5 ml CHCl_3 . The combined filtrates are evaporated to dryness, producing an orange solid which is recrystallized by vapour diffusion of Et_2O in a chloroform solution, yielding a yellow solid. Yield 132 mg (82%). $^1\text{H NMR}$ (CDCl_3): δ 1.83 (s, 15H, Cp^*), 3.47 (s, 3H, CH_3), 3.76 (s, 3H, CH_3) 7.10 (m, 1H, *m*-CH pyr), 7.85 (m, 1H, *p*-CH pyr), 8.45 (d, $J=5.8$ Hz, 1H, *m*-CH pyr), 9.62 (d, $J=8.6$ Hz, 1H, *o*-CH pyr). $^{13}\text{C NMR}$ (CDCl_3): δ 8.5 (Cp^*), 28.8 (CH_3), 31.9 (CH_3), 94.4 (Cp^*), 107.1 (NC(CO)), 116.3 (pyr), 124.6 (pyr), 142.6 (pyr), 144.8 (pyr), 149.7 (pyr), 152.1 (CO), 152.7 (NCN), 153.4 (CO), 173.9 (C-Ir). Elemental analysis (%) calc for $\text{C}_{22}\text{H}_{25}\text{N}_5\text{O}_2\text{IrCl}$: C 42.68; H 4.07; N 11.31. Found: C 42.59; H 3.78; N 11.10. ESI-MS (CH_3CN , m/z): 584.2 [$\text{M}-\text{Cl}$] $^+$, 641.9 [$\text{M}+\text{Na}$] $^+$, 657.9 [$\text{M}+\text{K}$] $^+$, 1260.8 [$2\text{M}+\text{Na}$] $^+$.

Synthesis of complex **3H-Ir**. A solution was prepared by diluting 300 μl $\text{HBF}_4\text{:Et}_2\text{O}$ with dry CHCl_3 up to a total volume of 10 ml (2.2 mM HBF_4 solution). Complex **3-Ir** (41.0 mg, 0.066 mmol) was placed in a vial and dissolved in 0.5 ml dry CHCl_3 , 0.5 ml (1.312 mmol, 120 eq.) of the HBF_4 solution were then added to the solution of the complex. A yellow solid separated immediately. The solid was isolated by filtration and recrystallized from $\text{CH}_3\text{CN:Et}_2\text{O}$. Yield 30.9 mg (75%). $^1\text{H NMR}$ (CD_3CN): δ 1.85 (s, 15H, Cp^*), 3.42 (s, 3H, CH_3), 3.70 (s, 3H, CH_3) 7.54 (m, 1H, *m*-CH pyr), 8.21 (m, 1H, *p*-CH pyr), 8.62 (m, 1H, *m*-CH pyr), 9.77 (m, 1H, *o*-CH pyr), 11.60 (s, 1H, NH). $^{13}\text{C NMR}$ (CD_3CN): δ 9.4 (Cp^*), 29.8 (CH_3), 32.9 (CH_3), 95.4 (Cp^*), 117.1 (NC(CO)), 125.5 (pyr), 143.5 (pyr), 145.5 (pyr), 150.6 (pyr), 152.90 (CO), 153.5 (NCN), 154.2 (CO), 174.7 (C-Ir). Elemental analysis calc for $\text{C}_{22}\text{H}_{26}\text{N}_5\text{O}_2\text{IrClBF}_4$: C 37.38; H 3.71; N 9.91. Found: C 37.00; H 3.68; N 9.23. ESI-MS (CH_3CN , m/z): 584.2 [$\text{M}-\text{HCl}-\text{BF}_4$] $^+$, 619.9 [$\text{M}-\text{BF}_4$] $^+$, 1238.3 [$2\text{M}-\text{HBF}_4-\text{BF}_4$] $^+$.

Deprotonation of complex **3H-Ir**. To a suspension of complex **3H-Ir** (30.9 mg, 0.049 mmol) in dry CHCl_3 (1 ml) was added a suspension of *t*-BuONa (5.1 mg, 0.05 mmol, 1 eq) in dry CHCl_3 (0.4 mL). The reaction mixture was stirred at room temperature for 3 hours, after which it was filtered over Celite. The solvent was evaporated to dryness yielding a yellow-orange solid which analyzed as complex **3-Ir**.

Deposition Numbers 2173460 (for **3-Ir**) and 2170918 (for **3H-Ir**) contain the supplementary crystallographic data for this paper. These data are provided free of charge by the joint Cambridge Crystallographic Data Centre and Fachinformationszentrum Karlsruhe Access Structures service www.ccdc.cam.ac.uk/structures.

Acknowledgements

Support by the Consorzio Interuniversitario per le Reattività Chimiche e la Catalisi (CIRCC) is gratefully acknowledged. We wish

to thank Dr. Maurizio Ballico, University of Udine, for support in performing the catalytic tests. Open Access funding provided by Università degli Studi di Padova within the CRUI-CARE Agreement.

Conflict of Interest

The authors declare no conflict of interest.

Data Availability Statement

The data that support the findings of this study are available in the supplementary material of this article.

Keywords: Adenine · Iridium · Metalation · Protic N-heterocyclic carbenes · Xanthine

- [1] a) *N-Heterocyclic Effective Tools for Organometallic Synthesis*, (Ed.: S. P. Nolan, Wiley-VCH, Weinheim, 2014); b) *N-Heterocyclic Carbenes: from Laboratory Curiosities to Efficient Synthetic Tools*, (Ed.: S. Díez-González), Royal Society of Chemistry, Cambridge, 2nd edn, 2017.
- [2] R. Breslow, *J. Am. Chem. Soc.* **1958**, *80*, 3719–3726.
- [3] a) M. J. Clarke, H. Taube, *J. Am. Chem. Soc.* **1975**, *97*, 1397–1403; b) L. G. F. Lopes, A. Wieraszko, Y. El-Sharif, M. J. Clarke, *Inorg. Chim. Acta* **2001**, *312*, 15–22.
- [4] a) S. H. Wiedemann, J. C. Lewis, J. A. Ellman, R. G. Bergman, *J. Am. Chem. Soc.* **2006**, *128*, 2452–2462; b) M. A. Esteruelas, F. J. Fernández-Alvarez, E. Oñate, *Organometallics* **2008**, *27*, 6236–6244; c) G. Song, Y. Su, R. A. Periana, R. H. Crabtree, K. Han, H. Zhang, X. Li, *Angew. Chem. Int. Ed.* **2010**, *49*, 912–917; *Angew. Chem.* **2010**, *122*, 924–929; d) A. R. Naziruddin, A. Hepp, T. Pape, F. E. Hahn, *Organometallics* **2011**, *30*, 5859–5866.
- [5] M. Leow, C. Ho, M. Gardiner, A. Bissember, *Catalysts* **2018**, *8*, 620.
- [6] a) D. Zhao, W. Wang, S. Lian, F. Yang, J. Lan, J. You, *Chem. Eur. J.* **2009**, *15*, 1337–1340; b) P. Xi, F. Yang, S. Qin, D. Zhao, J. Lan, G. Gao, C. Hu, J. You, *J. Am. Chem. Soc.* **2010**, *132*, 1822–1824; c) B. Liu, X. Qin, K. Li, X. Li, Q. Guo, J. Lan, J. You, *Chem. Eur. J.* **2010**, *16*, 11836–11839.
- [7] a) S. Kuwata, F. E. Hahn, *Chem. Rev.* **2018**, *118*, 9642–9677; b) M. C. Jahnke, F. E. Hahn, *Coord. Chem. Rev.* **2015**, *293–294*, 95–115.
- [8] a) H. J. Krentzien, M. J. Clarke, H. Taube, *Bioinorg. Chem.* **1975**, *4*, 143–151; b) M. J. Clarke, H. Taube, *J. Am. Chem. Soc.* **1975**, *97*, 1397–1403; c) A. Johnson, L. A. O'Connell, M. J. Clarke, *Inorg. Chim. Acta* **1993**, *210*, 151–157; d) C. Price, M. R. J. Elsegood, W. Clegg, N. H. Rees, A. Houlton, *Angew. Chem. Int. Ed. Engl.* **1997**, *36*, 1762–1764; e) A. Romerosa, J. Suarez-Varela, M. A. Hidalgo, J. C. Avila-Rosón, E. Colacio, *Inorg. Chem.* **1997**, *36*, 3784–3786; f) C. Price, M. A. Shipman, S. L. Gummerson, A. Houlton, W. Clegg, M. R. J. Elsegood, *J. Chem. Soc., Dalton Trans.* **2001**, 353–354; g) C. Price, M. A. Shipman, N. H. Rees, M. R. J. Elsegood, A. J. Edwards, W. Clegg, A. Houlton, *Chem. Eur. J.* **2001**, *7*, 1194–1201; h) D. Brackemeyer, A. Hervé, C. Schulte to Brinke, M. C. Jahnke, F. E. Hahn, *J. Am. Chem. Soc.* **2014**, *136*, 7841–7844; i) F. Kampert, D. Brackemeyer, T. T. Y. Tan, F. Ekkehardt Hahn, *Organometallics* **2018**, *37*, 4181–4185; j) M. I. P. S. Leitão, F. Herrera, A. Petronilho, *ACS Omega* **2018**, *3*, 15653–15656; k) T. T. Y. Tan, F. E. Hahn, *Organometallics* **2019**, *38*, 2250–2258; l) J. Blumenberg, L. F. B. Wilm, F. E. Hahn, *Organometallics* **2020**, *39*, 1281–1287; m) P. D. Dutschke, S. Bente, C. G. Daniliuc, J. Kinas, A. Hepp, F. E. Hahn, *Dalton Trans.* **2020**, *49*, 14388–14392; n) R. N. Osorio Yáñez, A. Hepp, T. T. Y. Tan, F. E. Hahn, *Organometallics* **2020**, *39*, 344–352.
- [9] K. Araki, S. Kuwata, T. Ikariya, *Organometallics* **2008**, *27*, 2176–2178.
- [10] a) F. E. Hahn, A. R. Naziruddin, A. Hepp, T. Pape, *Organometallics* **2010**, *29*, 5283–5288.
- [11] a) S. Kuwata, T. Ikariya, *Chem. Eur. J.* **2011**, *17*, 3542–3556; b) V. Miranda-Soto, D. B. Grotjahn, A. L. Cooksy, J. A. Golen, C. E. Moore, A. L. Rheingold, *Angew. Chem. Int. Ed.* **2011**, *50*, 631–635; *Angew. Chem.* **2011**, *123*, 657–661.

- [12] *Transition Metal Complexes of Naturally Occurring Nucleobases and Their Derivatives*; (Ed. J. R. Lusty); CRC Handbook of Nucleobase Complexes, Vol. I; CRC Press: Boca Raton, FL, 1990; pp 9–99.
- [13] a) H. Valdés, D. Canseco-González, J. M. Germán-Acacio, D. Morales-Morales, *J. Organomet. Chem.* **2018**, *867*, 51–54 and references cited therein; b) V. Stoppa, T. Scattolin, M. Bevilacqua, M. Baron, C. Graiff, L. Orian, A. Biffis, I. Menegazzo, M. Roverso, S. Bogialli, F. Visentin, C. Tubaro, *New J. Chem.* **2021**, *45*, 961–971; c) M. I. P. S. Leitão, C. Gonzalez, G. Francescato, Z. Filipiak, A. Petronilho, *Chem. Commun.* **2020**, *56*, 13365–13368; d) Q. Teng, Y. Zhao, Y. Lu, Z. Liu, H. Chen, D. Yuan, H. V. Huynh, Q. Meng, *Organometallics* **2022**, *41*, 161–168; e) J. Zhang, Md. M. Rahman, Q. Zhao, J. Feliciano, E. Bisz, B. Dziuk, R. Lalancette, R. Szostak, M. Szostak, *Organometallics* **2022**, *41*, 1806–1815; f) G. Francescato, S. M. da Silva, M. I. P. S. Leitão, A. Gaspar-Cordeiro, N. Giannopoulos, C. S. B. Gomes, C. Pimentel, A. Petronilho, *Applied Organomet. Chem.* **2022**, DOI 10.1002/aoc.6687.
- [14] a) C. S. Tiwari, P. M. Illam, S. N. R. Donthireddy, A. Rit, *Chem. Eur. J.* **2021**, *27*, 16581–16600; b) M. Iglesias, L. A. Oro, *Chem. Soc. Rev.* **2018**, *47*, 2772–2808.
- [15] R. Guan, L. Xie, L. Ji, H. Chao, *Eur. J. Inorg. Chem.* **2020**, 3978–3986.
- [16] D. Wang, D. Astruc, *Chem. Rev.* **2015**, *115*, 6621–6686.

Manuscript received: July 28, 2022
Revised manuscript received: October 7, 2022
Accepted manuscript online: October 7, 2022